

Additivity of Diene Substituent Gibbs Free Energy Contributions for Diels–Alder Reactions between $\text{Me}_2\text{C}=\text{CMe}_2$ and Substituted Cyclopentadienes

Austin S. Flemming, Brendan C. Dutmer,* and Thomas M. Gilbert*

Cite This: *ACS Omega* 2023, 8, 14160–14170

Read Online

ACCESS |



Metrics & More

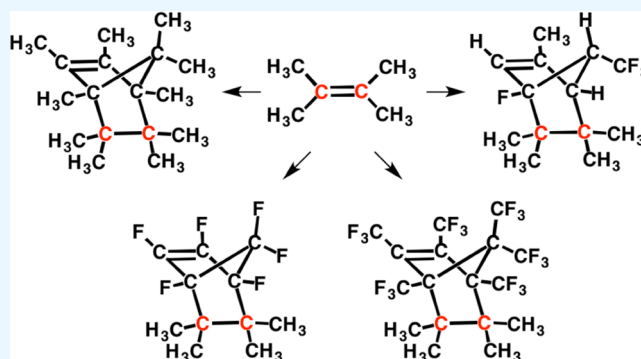


Article Recommendations



Supporting Information

ABSTRACT: Systematic computational studies of pericyclic Diels–Alder reactions between $(\text{H}_3\text{C})_2\text{C}=\text{C}(\text{CH}_3)_2$, **1**, and all permutations of substituted cyclopentadienes $c\text{-C}_5\text{R}^1\text{R}^2\text{R}^3\text{R}^4\text{R}^5\text{R}^6$ ($\text{R} = \text{H}, \text{CH}_3, \text{CF}_3, \text{F}$) allowed isolation of substitutional effects on Gibbs free energy barrier heights and reaction Gibbs free energies. “Average Substitution Gibbs Free Energy Correction” $\Delta G_{\text{ASC}\#}^{\ddagger}/\Delta G_{\text{ASC}\#}$ values for each substituent in each position appeared to be additive. Substituent effects on barriers showed interesting contrasts. Methyl substitution at positions 5a and 5b increased barriers significantly, while substitution at all other positions had essentially no impact. In contrast, fluoro substitution at positions 5a and 5b lowered barriers more than substitution at other positions. Trifluoromethyl substitution mixed these effects, in that substitution at positions 5a and 5b increased barriers, but substitution at other positions lowered them. Despite the variances, $\Delta G_{\text{ASC}\#}^{\ddagger}/\Delta G_{\text{ASC}\#}$ values allowed reliable prediction of barriers and exergonicities for reactions between **1** and highly substituted cyclopentadienes, and between **1** and cyclopentadienes with random mixtures of $\text{CH}_3/\text{CF}_3/\text{F}$ substituents. $\Delta G_{\text{ASC}\#}^{\ddagger}/\Delta G_{\text{ASC}\#}$ values were correlated with steric considerations and quantum theory of atoms in molecules (QTAIM) calculations. Overall, the ASC values provide a resource for predicting which Diels–Alder reactions of this type should occur at rapid rates and/or give stable bicyclic products.



INTRODUCTION

The Diels–Alder reaction is one of the most fundamental in organic chemistry, being both a textbook archetype¹ and a laboratory staple. Its utility and regioselectivities have engendered many experimental and computational studies of the reaction bases, with frontier molecular orbital theory playing a critical role in our understanding. Studies have clarified that transition state structures and energies play the most important roles in determining reaction outcomes, so focus on transition states has dictated most studies. Early studies^{2,3} that involved questions of orbital matching, radical vs closed-shell electronic interactions, and steric congestion have evolved to consider more complicated issues such as diradical mechanisms,^{4,5} Pauli repulsion,⁶ and catastrophe theory.⁷ Aspects and applications of the Diels–Alder reactions are reviewed regularly; recent reviews examined the role of the reaction in natural/biochemical systems,^{8,9} polymer synthesis,^{10,11} and click chemistry.^{12,13} Computational studies involving inverse electron demand,¹⁴ energy decomposition analysis,¹⁵ and molecular dynamics¹⁶ of the reaction have provided considerable insight into the fine details of cyclization.

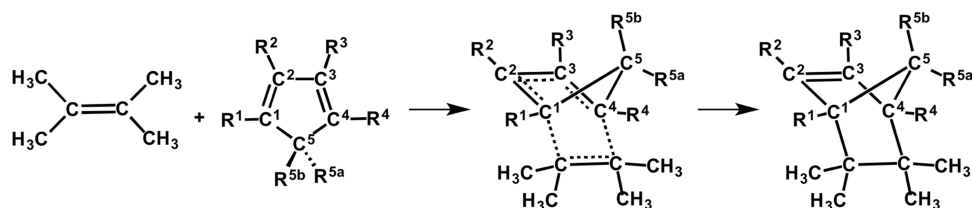
Cyclopentadienes represent common yet fascinating dienes in the Diels–Alder reaction,¹⁷ as they provide bicyclic products containing strained bridges. We recently reported computational studies of Diels–Alder-like reactions between the aminoborane dienophile $(\text{F}_3\text{C})_2\text{B}=\text{NMe}_2$ and all permutations of substituted cyclopentadienes $c\text{-C}_5\text{R}^1\text{R}^2\text{R}^3\text{R}^4\text{R}^5\text{R}^6$ ($\text{R} = \text{H}, \text{CH}_3, \text{CF}_3, \text{F}$).¹⁸ The data showed that, as in organic Diels–Alder reactions, the likelihood and regioselectivity of product formation were determined far more by transition state issues than thermodynamic ones. Notably, several transition state barriers and relative stabilities of product structures proved inconsistent with the regioselectivity “rules” applicable to organic systems. More importantly, we demonstrated that “Average Substitution Gibbs Free Energy Correction” $\Delta G_{\text{ASC}\#}^{\ddagger}/\Delta G_{\text{ASC}\#}$ for each substituent in each position provided insight into positional electronic effects.

Received: February 8, 2023

Accepted: March 28, 2023

Published: April 5, 2023



Scheme 1. Labeling Diagram for Diels–Alder Reactions Between **1** and Substituted Cyclopentadienes

That $\Delta G_{\text{ASC}\#}^{\ddagger}/\Delta G_{\text{ASC}\#}$ values were additive allowed predictions of efficacies for reactions between the aminoborane and cyclopentadienes with mixed substituents.

Given these findings, it seemed appropriate to perform a similar study involving an organic dienophile and cyclopentadienes (Scheme 1) and to examine whether substituent effects in such reactions were additive. More limited studies of substituent additivity in organic Diels–Alder reactions have appeared,^{19–28} but none explored all possible substitution permutations, refined additivity parameters, or explored dienes containing mixtures of electronically varied substituents. We, therefore, in this work computationally determined barrier and product energetics for all permutations of the reaction between $\text{Me}_2\text{C}=\text{CMe}_2$, **1**, and substituted cyclopentadienes $c\text{-C}_5\text{R}^1\text{R}^2\text{R}^3\text{R}^4\text{R}^{5a}\text{R}^{5b}$ ($\text{R} = \text{H}, \text{CH}_3, \text{CF}_3, \text{F}$). The data predicted that at least half of the reactions **1** + $c\text{-C}_5\text{H}_x\text{R}_{6-x}$ ($\text{R} = \text{CH}_3, \text{CF}_3$) and all of the reactions **1** + $c\text{-C}_5\text{H}_x\text{F}_{6-x}$ should be exergonic. Substituent effects on barriers showed interesting contrasts. Methyl substitution at positions 5a and 5b increased barriers significantly, while substitution at all other positions had essentially no impact. In contrast, fluoro substitution at positions 5a and 5b lowered barriers more than substitution at other positions. Trifluoromethyl substitution mixed these effects, in that substitution at positions 5a and 5b increased barriers, but substitution at other positions lowered them.

Despite the variances, we found that $\Delta G_{\text{ASC}\#}^{\ddagger}/\Delta G_{\text{ASC}\#}$ values for each substituent in each position were additive and allowed reliable predictions of barriers and exergonicities for reactions between **1** and highly substituted cyclopentadienes, removing the need for direct calculations. They also allowed prediction of energetics for Diels–Alder reactions between **1** and cyclopentadienes with random mixtures of $\text{CH}_3/\text{CF}_3/\text{F}$ substituents that agreed well with direct calculations, demonstrating that substituent additivity can be exploited for a range of substituted cyclopentadienes. $\Delta G_{\text{ASC}\#}^{\ddagger}/\Delta G_{\text{ASC}\#}$ values were correlated with steric considerations and QTAIM calculations. Overall, the ASC values provide a resource for predicting which Diels–Alder reactions of this type should occur at rapid rates and/or give stable bicyclic products.

COMPUTATIONAL METHODS

The Gaussian suite G09²⁹ was employed for all optimizations. For reactions between **1** and cyclopentadienes, component structures were initially optimized without constraints using either the M06-2X³⁰ or $\omega\text{B97X-D}$ ³¹ DFT models. A sizable integration grid (keyword Int = UltraFineGrid) and the 6-311+G(d,p) basis set were used throughout.^{32–34} Stationary point structures were then reoptimized using different DFT models to provide a sense of the range of energy values provided by different models for identical reactions³⁵ and to evaluate the effect of dispersion corrections.^{31,36} To provide perturbation theory checks on the DFT results for methyl- and

fluorocyclopentadiene reactions DLPNO-CCSD(T)//M06-2X+GD3I^{37–39} single-point energy determinations were performed on all reaction components using the ORCA program.^{40,41} These employed auxiliary basis sets for Coulomb and correlation corrections (autoaux keyword)^{42–44} and were also used to demonstrate that no RHF \rightarrow UHF instabilities existed in the reference wave functions. Plots of DFT vs DLPNO-CCSD(T) Gibbs free energy data are shown in the Supporting Information (Figure S1). All models gave reasonably linear agreement with the DLPNO-CCSD(T) data, with fitted line slopes near 1 and R values >0.99 . The y -intercepts were somewhat large (ca. -15 kJ mol^{-1}), denoting that the DFT energetics tended to be systematically higher than the DLPNO-CCSD(T) values. Judging by the fit parameters, the M06-2X+GD3 model gave the overall best agreement with the coupled cluster model. For this reason, the M06-2X+GD3 model is used below when discussing results for **1** + trifluoromethylcyclopentadienes, for which the DLPNO-CCSD(T) calculations proved too taxing for our resources.

To ensure that the DLPNO-CCSD(T) calculations did not suffer from basis set incompleteness using the 6-311+G(d,p) basis set, DLPNO-CCSD(T)/aug-cc-pVTZ//M06-2X+GD3 single point calculations were performed on several DA reactions between **1** and methyl- and fluorocyclopentadienes. The values obtained differed by no more than 7 kJ mol^{-1} from those employing the 6-311+G(d,p) basis set; we therefore believe that the original calculations are converged with respect to the basis set.

Frequency calculations were performed with all optimizations to confirm that ground states were minima (no imaginary frequencies) and that transition states were first-order saddle points (one imaginary frequency). M06-2X-derived Gibbs free energy corrections (ΔG_{298} , unscaled) were used to adjust raw energies (see the Supporting Information). We focused on Gibbs free energies rather than electronic energies because the combination reaction is better represented using Gibbs free energy comparisons that account for the loss of degrees of freedom in the transition state and product. That the transition states connected the relevant reactants and products was confirmed by visualizing the imaginary vibrations using GaussView⁴⁵ and WebMO.⁴⁶ The latter was used for molecular graphics in the figures below. Kaleidagraph for Macintosh⁴⁷ was used to generate energy data graphs and perform least-squares line determinations.

QTAIM charge data were obtained from calculations using M06-2X+GD3-level wave functions and the AIMAll program,⁴⁸ which implements the quantum theory of atoms in molecules (QTAIM) theory developed by Bader and co-workers.^{49–51}

“Average Substitution Corrections” (denoted $\Delta G_{\text{ASC}\#}^{\ddagger}$ and $\Delta G_{\text{ASC}\#}$ for Gibbs free energy barriers and reaction energies, respectively, with # representing the position of interest) were determined by treating the Gibbs free energy data as previously

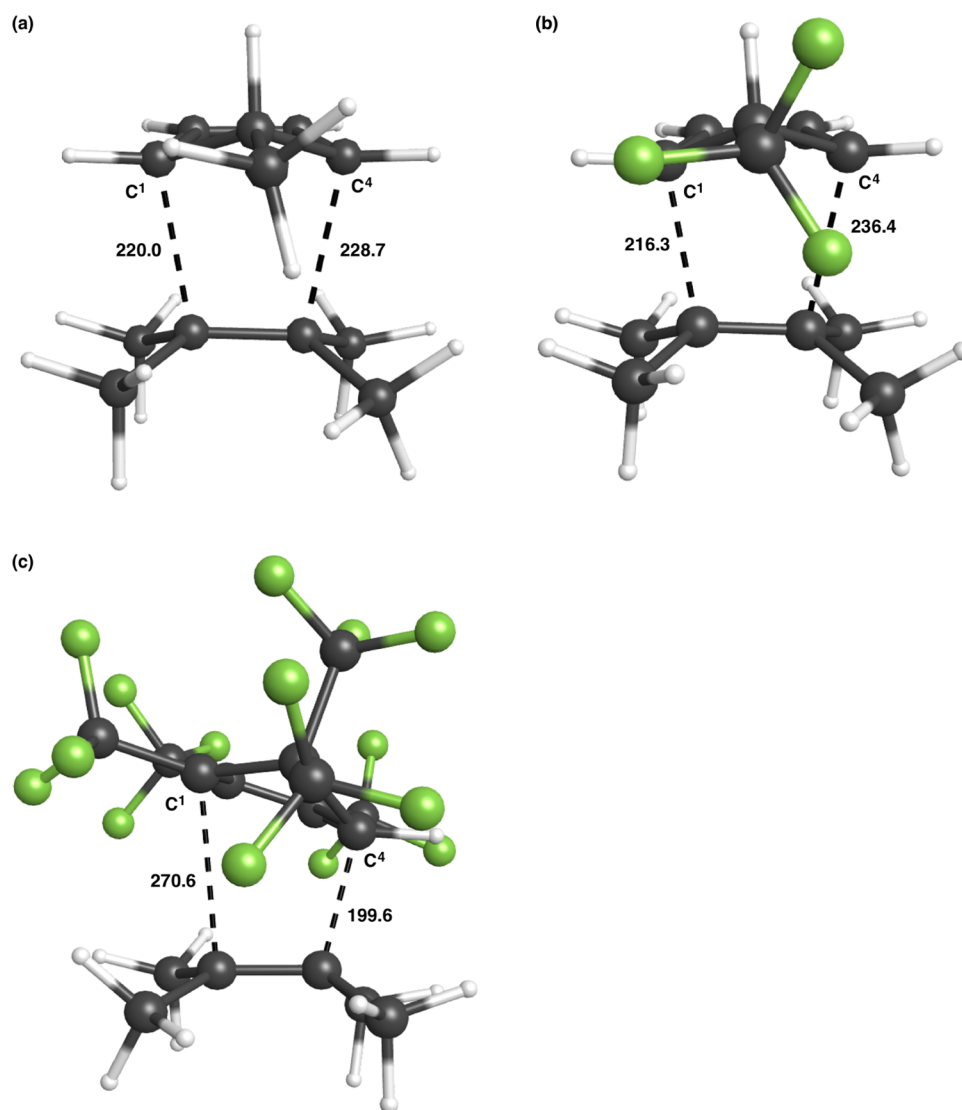


Figure 1. Predicted transition state geometries (M06-2X+GD3, distances in pm) for reactions between **1** and (a) *c*-5a-C₅H₅(CH₃); (b) *c*-5a-C₅H₅(CF₃); (c) *c*-1,2,3,5a,5b-C₅H(CF₃)₅. Carbons are black, fluorines are green, and hydrogens are white. Subfigures (a)–(c) show the effect of repulsions associated with the CR₃ R atom at position 5a on the C[⋯]C¹ and C[⋯]C⁴ forming distances. Subfigure (c) shows the extreme asymmetry of the transition state for the case.

described.¹⁸ Briefly, a substitution correction is the difference between an energy (barrier or overall reaction) determined for a Diels–Alder reaction for a cyclopentadiene with a particular substitution pattern and the energy determined for the reaction involving the cyclopentadiene with that pattern but lacking the substituent in the position of interest. $\Delta G_{\text{ASC}\#}^{\ddagger}/\Delta G_{\text{ASC}\#}$ is the average of all such substitution corrections for a particular substituent at a particular position. An example calculation is shown in the [Supporting Information](#). $\Delta G_{\text{ASC}\#}^{\ddagger}/\Delta G_{\text{ASC}\#}$ values adjust the energetics for the parent Diels–Alder reaction **1** + *c*-C₅H₆ based on the position(s) of substitution in the substituted cyclopentadiene and consequently act as proxies for the impact of substitution. Since they were derived from $\Delta G_{298}^{\ddagger}/\Delta G_{298}$ values, $\Delta G_{\text{ASC}\#}^{\ddagger}/\Delta G_{\text{ASC}\#}$ values are appropriate for T = 298K, but the temperature will not be referenced hereafter. $\Delta G_{\text{ASC}\#}^{\ddagger}/\Delta G_{\text{ASC}\#}$ calculations and associated standard deviations (σ)⁵² for all model chemistries are available in the [Supporting Information](#).

RESULTS AND DISCUSSION

Structural Issues. [Scheme 1](#) shows the labeling of the substituent positions. The product geometries were largely as expected, with the only notable features being that the C–CF₃ distances in moderately and highly substituted trifluoromethylbornenes were longer than typical (ca. 160–165 pm). The computationally predicted transition states were generally less symmetric than implied by the scheme. The differences between C[⋯]C forming distances in the transition states unsurprisingly reflected proximity to the methyl groups on **1**, with substitution at the 1/4 positions increasing the associated C[⋯]C distances more than did substitution at the 2/3 positions ([Table S1](#)). Substitution of CH₃ or CF₃ at position 5a increased the C[⋯]C distance of whichever carbon pair had the smaller C–C^{5a}–H/F torsional angle because the H/F was pointed toward the pair, causing steric repulsion ([Figure 1a,b](#)). In contrast, substitution of smaller fluorine at position 5a had essentially no impact on the forming distances. Substituents at position 5b did not significantly impact forming distances. On

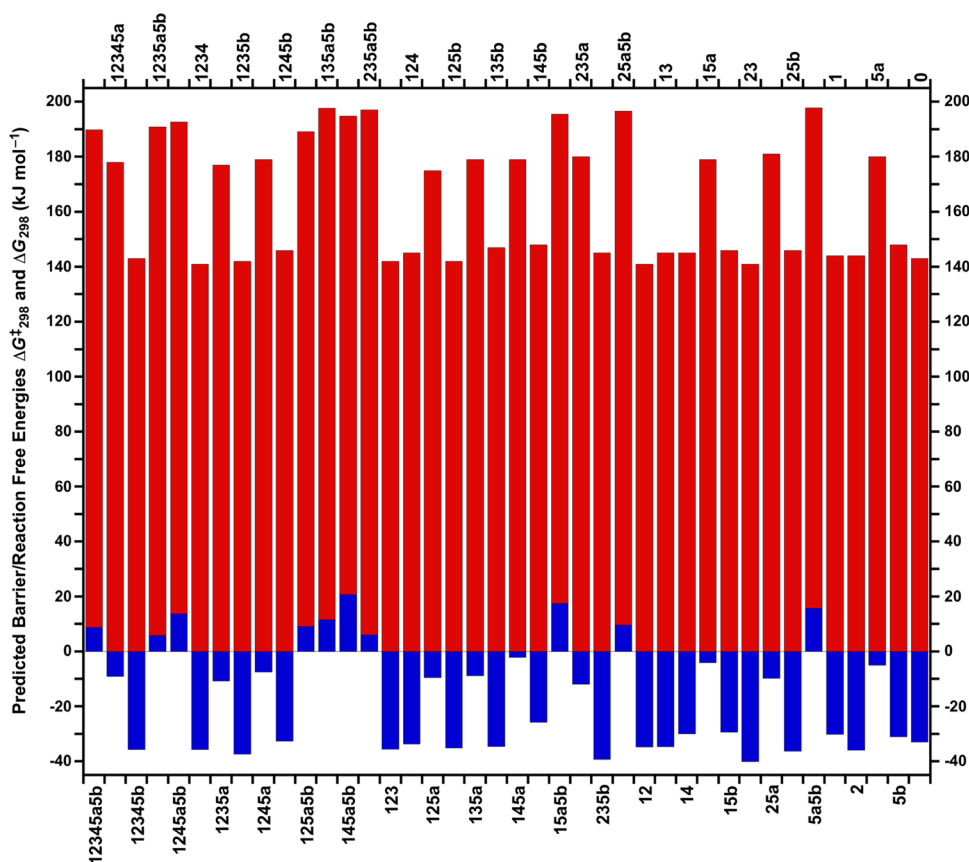


Figure 2. Predicted transition state Gibbs free energy barriers $\Delta G_{298}^{\ddagger}$ (red bars) and reaction Gibbs free energies ΔG_{298} (blue bars, DLPNO-CCSD(T)//M06-2X+GD3, kJ mol^{-1}) for all permutations of the Diels–Alder reaction **1** + $c\text{-C}_5\text{H}_x(\text{CH}_3)_{6-x}$. Numbers along the x -axis (top and bottom) give the substitution pattern (see Scheme 1). These alternate bottom/top in the order given in the tables in the Supporting Information. The column marked 0 gives data for the parent reaction **1** + $c\text{-C}_5\text{H}_6$.

average, the **1** + fluorocyclopentadiene transition states showed the greatest tendency to be concerted and synchronous, with average unsigned deviations between $\text{C}\cdots\text{C}^1$ and $\text{C}\cdots\text{C}^4$ forming distances being 40 and 75% smaller than those in the methyl- and trifluoromethyl-substituted cases, respectively (Table S1). Substitution of fluorine at position 2 caused decreases in the $\text{C}\cdots\text{C}^4$ forming distances in concert with increased $\text{C}\cdots\text{C}^1$ forming distances with respect to those in the parent transition state, while simultaneously substituting fluorine at positions 1 and 3 caused the opposite. The latter is the dominant effect; for example, in the transition states for **1** + 1,2,3,5a- $\text{C}_5\text{F}_4\text{H}_2$ and **1** + 1,2,3,5b- $\text{C}_5\text{F}_4\text{H}_2$, the $\text{C}\cdots\text{C}^4$ forming distances are ca. 9 pm longer than the $\text{C}\cdots\text{C}^1$ forming distances. More symmetric transition states for CH_3 , CF_3 , and F occurred for some substitution patterns, including 5b-, 1,4-, and 2,3-substitution.

Interestingly, the one-third substituent effect appeared limited to the fluoro case. For example, consider the various cases of **1** + 1,3,5a,5b- $\text{C}_5\text{R}_4\text{H}_2$ transition states. The methyl-substituted transition state is nearly symmetric with bond-forming distances, only differing by 3 pm. The trifluoromethyl-substituted case, however, has the $\text{C}\cdots\text{C}^4$ distance 51 pm shorter than the $\text{C}\cdots\text{C}^1$ distance, while the fluoro-substituted case has the $\text{C}\cdots\text{C}^4$ bond-forming distance 26 pm longer than the $\text{C}\cdots\text{C}^1$ distance. These observations point to competition between electron and steric effects that will be explored further below.

Compared to our previous work involving $(\text{F}_3\text{C})_2\text{B}=\text{NMe}_2$ + substituted cyclopentadienes, the **1** + fluorocyclopentadiene transition states are more symmetric than the aminoborane hetero-Diels–Alder analogues. Additionally, the uniquely long bond-forming distances exhibited by the fluoro-substituted aminoborane transition states are not present in the carbon ring transition states.

The greater steric bulk of CF_3 vs H/F/ CH_3 meant transition states for **1** + trifluoromethylcyclopentadiene reactions showed the largest differences between $\text{C}\cdots\text{C}$ forming distances, with the **1** + c -1,2,3,5a,5b- $\text{C}_5\text{H}(\text{CF}_3)_5$ transition state exhibiting the largest difference of 71 pm (Figure 1c). While the reaction process for this combination and similar ones appears highly asynchronous, the models nonetheless suggest that all of these Diels–Alder reactions are concerted.

Parent Reaction. Very few uncatalyzed thermal Diels–Alder reactions involving **1** as the dienophile have appeared.^{53,54} To the best of our knowledge, the Diels–Alder reaction **1** + $c\text{-C}_5\text{H}_6$ has not been reported. The product norbornene was prepared through reduction of the relevant ditosylate.⁵⁵ The computational models indicate that the barrier is significant at $\Delta G_{298}^{\ddagger} = 141 \text{ kJ mol}^{-1}$, but product formation is exergonic at $\Delta G_{298} = -36 \text{ kJ mol}^{-1}$. It is thus possible that the reaction could occur at elevated temperatures.

In our previous work, we discovered that the Diels–Alder reaction between $(\text{F}_3\text{C})_2\text{B}=\text{NMe}_2$ and 1,3-butadiene was far more efficacious than that between $(\text{F}_3\text{C})_2\text{B}=\text{NMe}_2$ and 1,3-cyclopentadiene. It seemed worthy to determine whether a

similar result held here. Bachrach and White calculated the energetics of **1** + 1,3-butadiene at the MP4SDTQ/6-31G(d)//B3LYP/6-31G(d) level.⁵⁶ Reoptimizing their structures and determining Gibbs free energies gave $\Delta G_{298}^{\ddagger} = 151 \text{ kJ mol}^{-1}$ and $\Delta G_{298} = -116 \text{ kJ mol}^{-1}$ (DLPNO-CCSD(T)//M06-2X+GD3). The similar barriers between the **1** + *c*-C₅H₆ and **1** + 1,3-butadiene reactions indicate both should be similarly viable; the difference in product stabilities probably arises from the strain present in the norbornene.

1 + Methylcyclopentadienes. We begin with these since they differ from the others by involving an ene and dienes with electron-donating substituents. Fleming's analysis⁵⁷ of such systems indicates likelihoods of higher barriers than for the parent reaction and "meta" regioselectivities in the transition states and products. As the alkene is symmetric, the latter issue was not examined in this work. Figure 2 shows the Gibbs free energy barrier heights and reaction Gibbs free energies for Diels–Alder reactions between **1** and all permutations of methylcyclopentadienes in bar graph format. One sees that about half of the reactions are endergonic; the most endergonic have substitution at position 5a in common. This almost certainly arises from steric repulsions between this methyl group and those on the original ene moiety (Scheme 1). Consequently, if the barriers can be surmounted, a number of polymethylnorbornenes should be experimentally accessible. That said, the barrier values indicate that surmounting them will prove difficult. None are much smaller than that of the parent reaction, and several are considerably larger. Inspection shows that, again, substitution at position 5a creates the biggest problem, adding 40 kJ mol⁻¹ to the barrier in the case of **1** + *c*-5a-C₅H₅(CH₃). We note here Levandowski et al.'s recent study of Diels–Alder reactions between highly methyl-substituted cyclopentadienes and maleimide or ethene. The work agrees that substitution at the 5 position raises barriers and lowers experimental reaction rates, phenomena they attribute to angle distortions at the saturated carbon and associated repulsions.⁵⁸

The $\Delta G_{\text{ASC}\#}^{\ddagger}/\Delta G_{\text{ASC}\#}$ values (Table 1) support these points, adding a subtle effect for substitution at position 5b. One sees

Table 1. Calculated $\Delta G_{\#-0}^{\ddagger}/\Delta G_{\#-0}$ and $\Delta G_{\text{ASC}\#}^{\ddagger}/\Delta G_{\text{ASC}\#}$ values (DLPNO-CCSD(T)//M06-2X+GD3 for R = CH₃, F; M06-2X+GD3 for R = CF₃; kJ mol⁻¹) from all permutations of Diels–Alder reactions **1** + *c*-C₅H_xR_{6-x} (R = CH₃, F, CF₃)^a

substituent position	R = CH ₃		R = F		R = CF ₃	
	$\Delta G_{\text{ASC}\#}^{\ddagger}$	$\Delta G_{\text{ASC}\#}$	$\Delta G_{\text{ASC}\#}^{\ddagger}$	$\Delta G_{\text{ASC}\#}$	$\Delta G_{\text{ASC}\#}^{\ddagger}$	$\Delta G_{\text{ASC}\#}$
1	-1	2	-12	-28	-6	-8
2	-1	-4	-3	-5	-11	-12
3	-1	-4	-3	-5	-11	-12
4	-1	2	-12	-28	-6	-8
5a	42	36	-4	-16	59	60
5b	9	10	-2	-12	11	22

^aPositions 3 and 4 are identical by symmetry to positions 2 and 1, respectively.

that substitution at diene positions 1–4 has essentially no impact on the barriers or exergonicities, while substitution at position 5a raises the barriers and lowers the exergonicities by 42 and 36 kJ mol⁻¹, respectively. Substitution at position 5b raises both by ca. 10 kJ mol⁻¹, likely not enough to change the kinetics of cyclization much from the parent reaction (given

that this already has a high barrier), or the exergonicity enough to change a reaction from exergonic to endergonic.

Least-squares comparisons between calculated $\Delta G^{\ddagger}/\Delta G$ values and those determined by summing appropriate $\Delta G_{\text{ASC}\#}^{\ddagger}$ and $\Delta G_{\text{ASC}\#}$ values show the latter predict the former well (Figure S2). The barriers are particularly well modeled, with a line slope of 1.04, indicating that summing $\Delta G_{\text{ASC}\#}^{\ddagger}$ values should prove useful in predicting reaction kinetics. The barrier *y*-intercept being -8.9 kJ mol^{-1} implies a slight scaling error, but given that all of the barriers are greater than 140 kJ mol⁻¹, the effect of this on predictions of experimental viability is minimal.

It is interesting that placing methyl groups at ring positions 1 and 4 has little effect on the barriers and product Gibbs free energies. One anticipates at least a modest steric interaction between the alkene methyl substituents and these. Inspection of the structures shows no H...H interactions shorter than 225 pm for either the transition state or product. This value approximates the sum of the van der Waals radius for hydrogen, so apparently, it is sufficiently long to avoid repulsions that raise the relevant Gibbs free energies.

It intrigued us that $\Delta G_{\text{ASC}1}^{\ddagger}$ and $\Delta G_{\text{ASC}2}^{\ddagger}$ were equal, in contrast to the comparisons for the other rings (Table 1). We probed this by determining QTAIM charges on C1 and C2 in the free methylcyclopentadienyl rings and in the transition states for the **1** + *c*-*n*-C₅H₅(CH₃) (*n* = 1, 2) reactions (Table 2). One sees that the charges on the relevant ring carbons in the transition states differ little from those in the free rings. It appears that placing a methyl group at position 1 increases the negative charge at position 2 and vice versa. However, the charges are so small as to likely not create a transition state preference, meaning that the $\Delta G_{\text{ASC}1}^{\ddagger}$ and $\Delta G_{\text{ASC}2}^{\ddagger}$ should also be small and similar, as observed.

1 + Fluorocyclopentadienes. This case typifies Fleming's "electron-rich ene/electron-poor diene" case, expected to exhibit lower barriers than for the parent reaction and "ortho/para" regioselectivities.⁵⁸ The bar graph in Figure 3 shows the Gibbs free energy barrier heights and reaction Gibbs free energies for Diels–Alder reactions between **1** and all permutations of fluorocyclopentadienes. All of the reactions are exergonic, with reaction Gibbs free energy values ranging from ~ -30 to -120 kJ mol^{-1} . The fluoro-substituted species react with far greater exergonicity than the methyl- or trifluoromethyl-substituted species. Similar behavior was predicted for the aminoborane hetero-Diels–Alder analogues; however, the carbon-bridged products are dramatically more exergonic (ca. $> 50 \text{ kJ mol}^{-1}$).

Fluorine substitution at position 1 significantly lowers product Gibbs free energies ($\Delta G_{\text{ASC}1} = -28 \text{ kJ mol}^{-1}$, Table 2). Substitution at positions 5a and 5b also lower product Gibbs free energies ($\Delta G_{\text{ASC}5a} = -16 \text{ kJ mol}^{-1}$, $\Delta G_{\text{ASC}5b} = -12 \text{ kJ mol}^{-1}$). For reference, fluorine substitution at positions 4 (identical to position 1 by symmetry in the all-carbon rings) and 5b yielded similar results in the aminoborane hetero-Diels–Alder analogues ($\Delta G_{\text{ASC}4} = -24 \text{ kJ mol}^{-1}$, $\Delta G_{\text{ASC}5b} = -8 \text{ kJ mol}^{-1}$).

The Gibbs free energy barriers range from ~ 100 to 140 kJ mol^{-1} . The barriers decrease as fluorine substitution increases, demonstrating that fluorines increase the Lewis acidity of the ring. The barriers for the aminoborane hetero-Diels–Alder analogues are lower than for the carbon-bridged products (ca. $> 30 \text{ kJ mol}^{-1}$).

Table 2. QTAIM Charges (M06-2X+GD3 wave functions, e^-) for free rings and for binding atoms in transition states of Diels–Alder reactions **1** + c - n - C_5H_5R ($R = CH_3, CF_3, F$)

	$q(C^1)$	$q(C^2)$		$q(C^1)$	$q(C^2)$
c -1- $C_5H_5(CH_3)$	-0.02	-0.05	c -2- $C_5H_5(CH_3)$	-0.06	-0.02
1 + c -1- $C_5H_5(CH_3)$ TS	-0.02	-0.04	1 + c -2- $C_5H_5(CH_3)$ TS	-0.05	-0.01
c -1- C_5H_5F	0.49	0.00	c -2- C_5H_5F	-0.01	0.49
1 + c -1- C_5H_5F TS	0.50	-0.02	1 + c -2- C_5H_5F TS	-0.02	0.48
c -1- $C_5H_5(CF_3)$	0.00	0.00	c -2- $C_5H_5(CF_3)$	-0.01	0.00
1 + c -1- $C_5H_5(CF_3)$ TS	0.00	-0.01	1 + c -2- $C_5H_5(CF_3)$ TS	-0.01	0.00

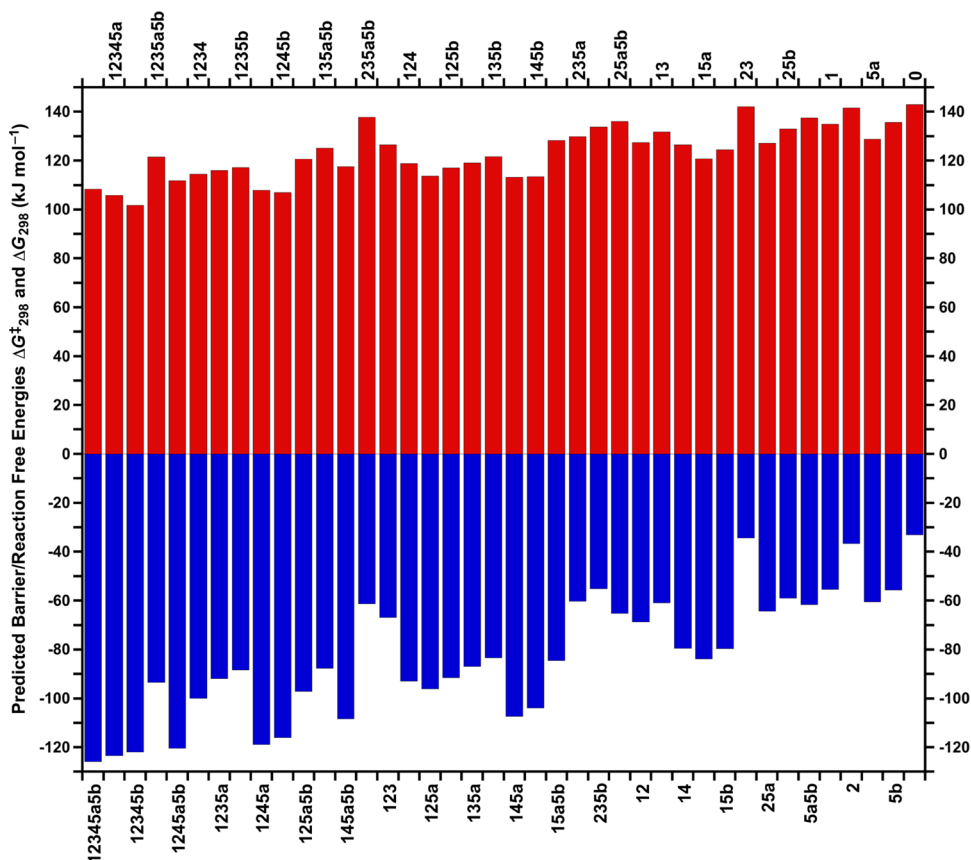


Figure 3. Predicted transition state Gibbs free energy barriers $\Delta G_{298}^{\ddagger}$ (red bars) and reaction Gibbs free energies ΔG_{298} (blue bars, DLPNO-CCSD(T)//M06-2X+GD3) (kJ mol^{-1}) for all permutations of the Diels–Alder reaction **1** + c - $C_5H_5F_{6-x}$. Numbers along the x -axis (top and bottom) give the substitution pattern (see Scheme 1). These alternate bottom/top in the order given in the tables in the Supporting Information. The column marked 0 gives data for the parent reaction **1** + c - C_5H_6 .

Fluorine substitution at all positions is predicted to lower Gibbs barrier energies, with only position 1 doing so significantly ($\Delta G_{\text{ASC1}^{\ddagger}} = -12 \text{ kJ mol}^{-1}$, Table 1). Dissimilarly, fluorine substitution at positions 1, 3, 5a, and 5b all increased the barrier energy in the aminoborane hetero-Diels–Alder analogues. Overall, although the **1** + fluorocyclopentadiene reactions are thermodynamically favorable, they exhibit relatively large kinetic barriers. The barriers may be partially overcome by fluorine substitution. Reactions with methyl- or trifluoromethyl groups are far less likely to be thermodynamically favorable; however, some of the trifluoromethyl substitutions result in exergonic reactions having barriers on the order of the fluoro-substitutions.

QTAIM charges on C1 and C2 (Table 2) indicate that the electron-withdrawing nature of fluorine induces a positive charge (≈ 0.5) upon either carbon to which it is attached. When the charge on C1 is more positive, the diene becomes more electrophilic at the C1 position, and the barrier is

lowered in a reverse-demand reaction. When the charge on C2 is positive due to fluorine bonding, the charge on the adjacent C1 is near-zero, and thus there is no predicted barrier lowering. There is a clear electronic preference that occurs for fluorine substitution at the 1/4 positions, which correlates with our finding that $\Delta G_{\text{ASC1}^{\ddagger}}$ is more negative than $\Delta G_{\text{ASC2}^{\ddagger}}$ (Table 1). The $\Delta G_{\text{ASC5a}^{\ddagger}}$ and $\Delta G_{\text{ASC5b}^{\ddagger}}$ values suggest that fluorine addition at the 5a and 5b positions, similar to position 2, does not increase the Lewis acidity of C1 much, if at all.

1 + Trifluoromethylcyclopentadienes. The trifluoromethyl group is regarded as a pure σ -withdrawing substituent, contrasted with fluoro groups that are σ -withdrawing but can be π -donating to a conjugated system.^{59,60} Fleming's analysis categorizes trifluoromethylcyclopentadienes as electronically related to fluorocyclopentadienes,⁵⁸ but of course, one must add the significant steric component associated with the bulky trifluoromethyl groups. Gibbs free energy barrier heights and reaction Gibbs free energies for all permutations are shown in

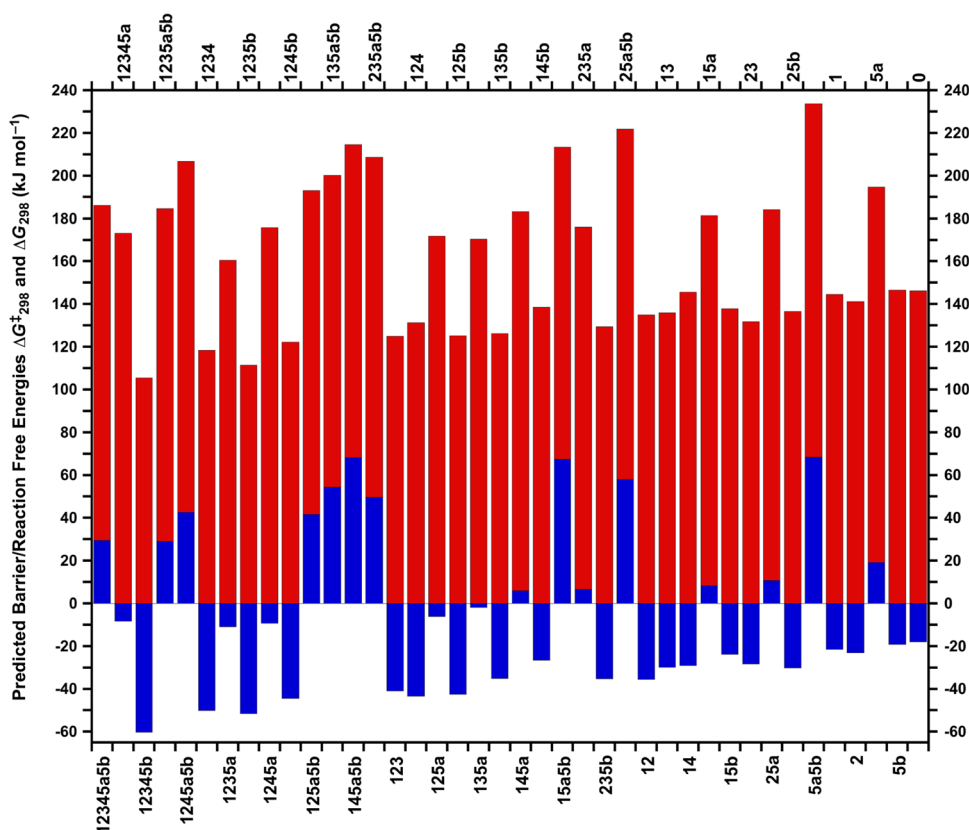


Figure 4. M06-2X+GD3-predicted transition state Gibbs free energy barriers $\Delta G_{298}^{\ddagger}$ (red bars) and reaction Gibbs free energies ΔG_{298} (blue bars, kJ mol^{-1}) for all permutations of the Diels–Alder reaction **1** + $c\text{-C}_5\text{H}_4(\text{CF}_3)_{6-x}$. Numbers along the x -axis (top and bottom) give the substitution pattern (see Scheme 1). These alternate bottom/top in the order given in the Supporting Information. The column marked 0 gives data for the parent reaction **1** + $c\text{-C}_5\text{H}_6$.

Figure 4. Approximately half of the reactions are exergonic, with substitution at the 5a position clearly increasing the endergonicities. In contrast to reactions between **1** and methylcyclopentadienes, some reactions here exhibit barriers lower than that of the parent reaction and distinct exergonicities. Thus, performing successful experimental reactions between **1** and trifluoromethylcyclopentadienes appears possible.

Inspection of the $\Delta G_{\text{ASC}\#}^{\ddagger}$ values (Table 1) shows agreement with and differences from those for the methyl-substituted cases. Substitution at position 5a still has the largest impact, adding 59 kJ mol^{-1} to the parent barrier. Substitution at 5b also raises the barriers but to a significantly smaller degree. Substitution at ring positions 1/2/3/4 lowers the barriers. In contrast to the fluorocyclopentadiene cases, substitution at the 2/3 positions lowers the barriers more than substitution at the 1/4 positions.

The least-squares lines (Figure S4) show that the $\Delta G_{\text{ASC}\#}^{\ddagger}$ and $\Delta G_{\text{ASC}\#}$ values additively predict barriers and reaction energies reasonably. The line slopes lie closer to 1.0 than for the methyl- and fluoro- cases, but the R values average 0.93. We suspect that some interatomic $\text{H}\cdots\text{F}$ interactions are not as well modeled as might be wished by the additivity approach, leading to scatter among the data. That said, the maximum difference between calculated and additivity-predicted barriers was 18 kJ mol^{-1} . We suspect that this would prove less than experimental error for thermodynamic measurements on many of these reactions.

Comparing the $\Delta G_{\text{ASC}\#}^{\ddagger}$ values for **1** + trifluoromethylcyclopentadienes with those for **1** + fluorocyclopentadienes reveals an interesting anomaly. The former show greater barrier lowering for a substituent at the 2/3 positions, while the latter show this for the 1/4 positions. QTAIM charge data provide a plausible explanation (Table 2). Fascinatingly, despite the electron-withdrawing nature of the CF_3 group, cyclopentadiene carbons to which it is attached carry no charge, either in the free ring or the reaction transition state. This recalls the result for **1** + methylcyclopentadienes above. If no electronic preference exists for the transition states, the preference observed must arise from steric effects. A trifluoromethyl substituent at position 2 is less sterically demanding in the transition state than one at position 1, so we believe this accounts for the preference.

1 + Mixed-Substituent Cyclopentadienes. To assess whether prediction of substituent additivity has a practical use, we used the random number generator function in Microsoft Excel to create 12 randomly substituted cyclopentadiene rings with the requirement that at least three of the four types be present in each ring. Energetics of the transition states and products for Diels–Alder reactions between **1** and these rings appear in Table 3, along with those predicted by summing appropriate $\Delta G_{\text{ASC}\#}^{\ddagger}/\Delta G_{\text{ASC}\#}$ values. One sees that the ASC-based predictions are generally good: the average absolute deviations for barriers and overall energies are $5/8 \text{ kJ mol}^{-1}$, respectively, while the corresponding root-mean-square errors are $6/9 \text{ kJ mol}^{-1}$. This demonstrates that $\Delta G_{\text{ASC}\#}^{\ddagger}/\Delta G_{\text{ASC}\#}$ values for different substituent types can combine to predict

Table 3. M06-2X+GD3-optimized $\Delta G_{298}^{\ddagger}/\Delta G_{298}$ values and $\Delta G_{298}^{\ddagger}/\Delta G_{298}$ values predicted (marked with “(p)”) by summing $\Delta G_{ASC\#}^{\ddagger}/\Delta G_{ASC\#}$ values (kJ mol^{-1}) 1 + *c*- $\text{C}_5(\text{R}^1)(\text{R}^2)(\text{R}^3)(\text{R}^4)(\text{R}^{5a})(\text{R}^{5b})$ (R = H, CH_3 , CF_3 , F; random substituents at random positions)^a

ring	$\Delta G_{298}^{\ddagger}$	ΔG_{298}	$\Delta G_{298}^{\ddagger}(\text{p})$	$\Delta G_{298}(\text{p})$
<i>c</i> -2- CH_3 -1- CF_3 -4-F- C_5H_3	82	-6	75	-20
<i>c</i> -5b- CH_3 -4- CF_3 - C_5H_4	93	36	95	43
<i>c</i> -5a- CH_3 -5b- CF_3 -4-F- C_5H_3	123	72	128	68
<i>c</i> -4- CH_3 -3- CF_3 -5a-F- C_5H_3	71	1	70	6
<i>c</i> -2- CF_3 -5b-F- C_5H_4	108	-1	107	6
<i>c</i> -5a- CH_3 -1- CF_3 -4-F- C_5H_3	124	33	130	36
<i>c</i> -4- CH_3 -1- CF_3 - C_5H_4	94	24	87	18
<i>c</i> -3- CH_3 -5b-F- C_5H_4	84	-5	85	3
<i>c</i> -5b- CH_3 -5a- CF_3 -2-F- C_5H_3	172	122	163	109
<i>c</i> -1- CH_3 -4- CF_3 -5b-F- C_5H_3	109	26	105	28
<i>c</i> -2- CH_3 -3- CF_3 -1-F- C_5H_3	92	10	81	-3
<i>c</i> -5a- CH_3 -1- CF_3 -3-F- C_5H_3	152	54	159	68
AAD			5	8
RMS			6	9

^aAAD = average absolute deviation; RMS = root-mean-square deviation.

energetics for reactions between **1** and a range of substituted cyclopentadienes.

Aminoborane Reactions Revisited. At the completion of our previous work on cyclopentadiene/aminoborane Diels–Alder reactions, we questioned whether the results and implications would allow us to predict and understand the behavior of analogous reactions using alkenes. The $\Delta G_{ASC\#}^{\ddagger}/\Delta G_{ASC\#}$ values are useful but are relative to the baseline parent reaction, and so do not directly characterize reaction viability. We decided a quantitative study was necessary to elucidate the trends further. Upon comparison of reaction Gibbs free energies, it is immediately apparent that differences in reaction viability are represented in values rather than trends. For the aminoborane systems, all but six reactions involving fluorocyclopentadienes and approximately one-third of those involving methylcyclopentadienes showed exergonic Gibbs free energies. For the alkene systems in this work, all reactions involving fluorocyclopentadienes and three-fourths of those involving methylcyclopentadienes are predicted to be exergonic. This indicates generally increased spontaneity for the alkene reactions, which probably reflects both the decreased steric bulk of **1** vs $(\text{F}_3\text{C})_2\text{B}=\text{NMe}_2$ and the weaker B ← N bond vs the C–C bond in the products. The significant differences are in the values; the extreme example is **1** + *c*- C_5F_6 (-115 kJ mol^{-1}) vs $(\text{F}_3\text{C})_2\text{B}=\text{NMe}_2$ + *c*- C_5F_6 (-20 kJ mol^{-1} ; M06-2X+GD3). Reactions involving trifluoromethylcyclopentadienes benefit from use of **1**, in that 60% of reactions **1** + *c*- $\text{C}_5(\text{CF}_3)_n\text{H}_{6-n}$ were predicted to be exergonic, while no reactions between $(\text{F}_3\text{C})_2\text{B}=\text{NMe}_2$ and *c*- $\text{C}_5(\text{CF}_3)_n\text{H}_{6-n}$ were.

Of course, viability for the Diels–Alder reaction usually depends more on barrier height than exergonicity, and here differences in barrier Gibbs free energies were apparent as well. It is worth recalling that the barrier heights for the parent reactions are notably different: 141 kJ mol^{-1} for **1** and 77 kJ mol^{-1} for $(\text{F}_3\text{C})_2\text{B}=\text{NMe}_2$. Consequently, the $\Delta G_{ASC\#}^{\ddagger}$ values for each do not encapsulate reaction viability from an experimenter’s point of view, as reactions involving the latter will be considerably faster. Overall, the aminoborane systems tend toward smaller barrier Gibbs free energies for all

substituents and substitutions. For example, the methyl- and fluorocyclopentadiene + $(\text{F}_3\text{C})_2\text{B}=\text{NMe}_2$ reactions exhibit barriers around 50 and 30 kJ mol^{-1} lower, respectively, than analogous reactions involving **1**. Considering all trends together, the most plausible combinations for successful Diels–Alder reactions involve $(\text{F}_3\text{C})_2\text{B}=\text{NMe}_2$ reacting with fluorocyclopentadienes owing to lowered reaction barriers coupled with exergonic reaction Gibbs free energies. Usefully, Diels–Alder reactions impracticable with alkenes may be viable with $(\text{F}_3\text{C})_2\text{B}=\text{NMe}_2$ and possibly other aminoboranes if they react more rapidly with dienes than themselves.

There were notable differences in $\Delta G_{ASC\#}^{\ddagger}/\Delta G_{ASC\#}$ values between the aminoborane and alkene systems (Table 4).

Table 4. Calculated $\Delta G_{ASC\#}^{\ddagger}/\Delta G_{ASC\#}$ values (M06-2X+GD3; kJ mol^{-1}) from all permutations of Diels–Alder reactions **1 + *c*- $\text{C}_5\text{H}_x\text{R}_{6-x}$ (R = CH_3 , F, CF_3) and $(\text{F}_3\text{C})_2\text{B}=\text{N}(\text{CH}_3)_2$ + *c*- $\text{C}_5\text{H}_x\text{R}_{6-x}$ (R = CH_3 , F, CF_3)**

substituent position	$\Delta G_{ASC\#}^{\ddagger}$ (C=C)	$\Delta G_{ASC\#}^{\ddagger}$ (B=N)	$\Delta G_{ASC\#}$ (C=C)	$\Delta G_{ASC\#}$ (B=N)
R = CH_3				
1	2	10	5	5
2	1	-11	-2	-9
3	1	-1	-2	0
4	2	-16	5	5
5a	43	44	37	47
5b	11	9	10	12
R = F				
1	-12	14	-26	1
2	-2	-8	-4	-3
3	-2	12	-4	8
4	-12	-17	-26	-24
5a	-10	8	-22	-4
5b	-3	9	-17	-8
R = CF_3				
1	-6	26	-8	2
2	-11	21	-12	3
3	-11	1	-12	-6
4	-6	9	-8	20
5a	59	85	60	89
5b	11	24	22	34

Trifluoromethyl groups had a dramatically large impeding effect on aminoborane reaction energetics, more so than on alkene reaction energetics. The effects were significantly higher for substitution at the 1, 2, and 5a positions, i.e., those that interact sterically with the aminoborane CF_3 substituents. Methyl substitution at the 2 and 4 ring positions resulted in lower transition state barriers for the aminoborane system relative to alkene values, while substitution at the 1 position gave higher barriers. We explained the unusual regiochemistries implied by the associated $\Delta G_{ASC\#}^{\ddagger}$ values in our previous paper; in short, they arise from the sizable polarity of $(\text{F}_3\text{C})_2\text{B}=\text{NMe}_2$, which is lost in **1**. The lower barriers result from electronic issues, while the higher one probably derives from the usual steric repulsions. Fluoro groups impeded the transition state barriers of the aminoborane system relative to the alkene system by 26 and 14 kJ mol^{-1} for the 1 and 3 substitutions, respectively. This inverts the results for methylcyclopentadienes and probably arises from the related electronic effects.

CONCLUSIONS

In this work, we used systematic computational studies of Diels–Alder reactions between symmetric $\text{Me}_2\text{C}=\text{CMe}_2$, **1**, and all permutations of substituted cyclopentadienes $c\text{-C}_5\text{R}^1\text{R}^2\text{R}^3\text{R}^4\text{R}^5\text{R}^6$ ($\text{R} = \text{H}, \text{CH}_3, \text{CF}_3, \text{F}$) to determine barrier heights and reaction energetics along with optimized structures. Both types of data showed interesting related features. Importantly, the data indicated that examples of all types of substituted cyclopentadienes should give cyclized products, even those with bulky trifluoromethyl substituents. This holds promise for preparation of an array of new norbornenes.

The energetic data were used to determine “Average Substitution Gibbs free energy Correction” $\Delta G_{\text{ASC}\#}^{\ddagger}/\Delta G_{\text{ASC}\#}$ values for each substituent type and position on the cyclopentadiene ring. Energetics predicted by summing $\Delta G_{\text{ASC}\#}^{\ddagger}/\Delta G_{\text{ASC}\#}$ values closely matched those from which they were derived, supporting the view that each substituent type and position contributes uniquely to the energetics and that the contributions are additive. The utility of this observation was confirmed by the good agreement between calculated and ASC-derived energetics for reactions between **1** and randomly multiply mixed-substituted cyclopentadienes. This means experimenters can determine in advance of synthesis whether a reaction involving **1** and a particularly substituted cyclopentadiene will react successfully. This means an array of specifically substituted norbornenes with desirable substitution patterns could become available.

We plan to examine whether regioselectivity can be accomplished in Diels–Alder reactions by placing CF_3 substituents on the alkene. This makes the alkene both bulkier and more Lewis acidic. Such substitution might create novel regioselectivity in the reaction. This could prove useful in areas like pharmaceutical synthesis, where regioselectivity is critical.

ASSOCIATED CONTENT

Supporting Information


The Supporting Information is available free of charge at <https://pubs.acs.org/doi/10.1021/acsomega.3c00831>.

Scatter plots and least-squares line fits for transition state barrier Gibbs free energy data; tables of $\Delta G_{\text{ASC}\#}^{\ddagger}/\Delta G_{\text{ASC}\#}$ values for all substituents and model chemistries; C–C forming distances in transition states; raw molecular energies of components and corrected relative Gibbs free energy barrier heights $\Delta G_{298}^{\ddagger}$ and reaction Gibbs free energies ΔG_{298} ; subtractions used to derive $\Delta G_{\text{ASC}\#}^{\ddagger}$ and $\Delta G_{\text{ASC}\#}$ values; $\Delta G^{\ddagger}/\Delta G$ values derived by summing $\Delta G_{\text{ASC}\#}^{\ddagger}/\Delta G_{\text{ASC}\#}$ values; and computed molecule Cartesian coordinates in a format for convenient visualization (PDF)

AUTHOR INFORMATION

Corresponding Authors

Brendan C. Dutmer – Department of Chemistry, Highland Community College, Freeport, Illinois 61032, United States; Email: Brendan.Dutmer@highland.edu

Thomas M. Gilbert – Department of Chemistry and Biochemistry, Northern Illinois University, DeKalb, Illinois 60115, United States;  orcid.org/0000-0003-2053-9655; Email: tgilbert@niu.edu

Author

Austin S. Flemming – Department of Chemistry, Highland Community College, Freeport, Illinois 61032, United States; Present Address: Department of Chemistry, University of Illinois, Chicago, Chicago, Illinois 60607, United States

Complete contact information is available at:

<https://pubs.acs.org/10.1021/acsomega.3c00831>

Notes

The authors declare no competing financial interest.

ACKNOWLEDGMENTS

This research did not receive any specific grant from funding agencies in the public, commercial, or not-for-profit sectors. The Northern Illinois University (NIU) Computational Chemistry Laboratory was created using funds from the U.S. Department of Education and is supported in part by the taxpayers of the State of Illinois. The work used resources of the Center for Research Computing and Data (CRCDD) at NIU, specifically the Gaea computer cluster. The authors thank Sergey Uzunyan and Dave Ulrick of CRCDD-NIU for their assistance and troubleshooting efforts. The authors also thank Highland Community College (HCC) Information Technology Services for equipment and service and the HCC Honors Program for providing undergraduate research opportunities.

REFERENCES

- (1) Carey, F. A.; Sundberg, R. J. *Advanced Organic Chemistry Part A: Structure and Mechanisms*; Springer Science + Business Media: New York, 2007, Chapter 10.2.
- (2) Houk, K. N. Generalized frontier orbitals of alkenes and dienes. Regioselectivity in Diels–Alder reactions. *J. Am. Chem. Soc.* **1973**, *95*, 4092–4094.
- (3) Houk, K. N. The Frontier Molecular Orbital Theory of Cycloaddition Reactions. *Acc. Chem. Res.* **1975**, *8*, 361–369.
- (4) Acocella, A.; Marforio, T. D.; Calvaresi, M.; Botoni, A.; Zerbetto, F. Electron Dynamics with Explicit-Time Density Functional Theory of the [4+2] Diels–Alder Reaction. *J. Chem. Theory Comput.* **2020**, *16*, 2172–2180.
- (5) Bartlett, P. D. 1,2- and 1,4-Cycloaddition to Conjugated Dienes. *Science* **1968**, *159*, 833–838.
- (6) Vermeeren, P.; Hamlin, T. A.; Bickelhaupt, F. M. Origin of asynchronicity in Diels–Alder reactions. *Phys. Chem. Chem. Phys.* **2021**, *23*, 20095–20106.
- (7) Ayarde-Henríquez, L.; Guerra, C.; Duque-Noreña, M.; Rincón, E.; Pérez, P.; Chamorro, E. Are There Only Fold Catastrophes in the Diels–Alder Reaction Between Ethylene and 1,3-Butadiene? *J. Phys. Chem. A* **2021**, *125*, 5152–5165.
- (8) Watanabe, K.; Sato, M.; Osada, H. Recent advances in the chemo-biological characterization of decalin natural products and unraveling of the workings of Diels–Alderase. *Fungal Biol. Biotechnol.* **2022**, *9*, 9.
- (9) Mastachi-Loza, S.; Ramirez-Candelero, T. I.; Benitez-Puebla, L. J.; Fuentes-Benites, A.; Gonzalez-Romero, C.; Vazquez, M. A. Chalcohes, a Privileged Scaffold: Highly Versatile Molecules in [4+2] Cycloadditions. *Chem. – Asian J.* **2022**, *17*, No. e202200706.
- (10) Gandini, A.; M Lacerda, T. Furan Polymers: State of the Art and Perspectives. *Macromol. Mater. Eng.* **2022**, *307*, No. 2100902.
- (11) Cadamuro, F.; Russo, L.; Nicotra, F. Biomedical Hydrogels Fabricated Using Diels–Alder Crosslinking. *Eur. J. Org. Chem.* **2021**, *2021*, 374–382.
- (12) Zhang, F.-G.; Chen, Z.; Tang, X.; Ma, J.-A. Triazines: Syntheses and Inverse Electron-demand Diels–Alder Reactions. *Chem. Rev.* **2021**, *121*, 14555–14593.

- (13) Neumann, K.; Gambardella, A.; Bradley, M. The emerging role of tetrazines in drug-activation chemistries. *ChemBioChem* **2019**, *20*, 872–876.
- (14) Deb, T.; Tu, J.; Franzini, R. M. Mechanisms and Substituent Effects of Metal-Free Bioorthogonal Reactions. *Chem. Rev.* **2021**, *121*, 6850–6914.
- (15) Sengupta, A.; Li, B.; Svatunek, D.; Liu, F.; Houk, K. N. Cycloaddition Reactivities Analyzed by Energy Decomposition Analyses and the Frontier Molecular Orbital Model. *Acc. Chem. Res.* **2022**, *55*, 2467–2479.
- (16) Houk, K. N.; Liu, F.; Yang, Z.; Seeman, J. I. Evolution of the Diels–Alder Reaction Mechanism since the 1930s: Woodward, Houk with Woodward, and the Influence of Computational Chemistry on Understanding Cycloadditions. *Angew. Chem., Int. Ed.* **2021**, *60*, 12660–12681.
- (17) Levandowski, B. J.; Raines, R. T. Click Chemistry with Cyclopentadiene. *Chem. Rev.* **2021**, *121*, 6777–6801.
- (18) Strominger, A. M.; Sutherland, B. L.; Flemming, A. S.; Dutmer, B. C.; Gilbert, T. M. Additivity of Diene Substituent Gibbs Free Energy Contributions for Diels–Alder Reactions between $(F_3C)_2B = NMe_2$ and Substituted Cyclopentadienes. *J. Phys. Chem. A* **2021**, *125*, 5456–5469.
- (19) Robiette, R.; Marchand-Brynaert, J.; Peeters, D. Influence of Diene Substitution on Transition State Stabilization in Diels–Alder Reaction. *J. Org. Chem.* **2002**, *67*, 6823–6826.
- (20) Qiu, Y. Substituent effects in the Diels–Alder reactions of butadienes, cyclopentadienes, furans and pyrroles with maleic anhydride. *J. Phys. Org. Chem.* **2015**, *28*, 370–376.
- (21) Perez, P.; Chamorro, E. Theoretical analysis of substituted Diels–Alder reagents to determine the polar or nonpolar character of the reaction. *Lett. Org. Chem.* **2011**, *8*, 88–94.
- (22) Mohajeri, A.; Shahamirian, M. Theoretical study of Diels–Alder reaction: role of substituent in regioselectivity and aromaticity. *J. Iran. Chem. Soc.* **2010**, *7*, 554–563.
- (23) Domingo, L. R.; Saez, J. A. Understanding the mechanism of polar Diels–Alder reactions. *Org. Biomol. Chem.* **2009**, *7*, 3576–3583.
- (24) Baki, S.; Maddaluno, J.; Derdour, A.; Chaquin, P. Diels–Alder Reactions of Symmetrically 1,4-Disubstituted Dienes: Theoretical Study on the Influence of the Configuration of the Double Bonds on the Regio- and Endoselectivity. *Eur. J. Org. Chem.* **2008**, *2008*, 3200–3208.
- (25) Schmidt, R. R. Hetero-Diels–Alder Reaction in Highly Functionalized Natural Product Synthesis. *Acc. Chem. Res.* **1986**, *19*, 250–259.
- (26) Singleton, D. A.; Redman, A. M. Vinylboranes as *trans*-Dihydroxyethylene Equivalents for Diels–Alder Reactions. *Tetrahedron Lett.* **1994**, *35*, 509–512.
- (27) Branchadell, V.; Sodupe, M.; Ortuño, R. M.; Oliva, A.; Gomez-Pardo, D.; Guingant, A.; d'Angelo, J. Diels–Alder Cycloadditions of Electron-Rich, Electron-Deficient, and Push-Pull Dienes with Cyclic Dienophiles: High-Pressure-Induced Reactions and Theoretical Calculations. *J. Org. Chem.* **1991**, *56*, 4135–4141.
- (28) Alston, P. V.; Ottenbrite, R. M.; Shillady, D. D. Secondary Orbital Interactions Determining Regioselectivity in the Diels–Alder Reaction. *J. Org. Chem.* **1973**, *38*, 4075–4077.
- (29) Frisch, M. J.; Trucks, G. W.; Schlegel, H. B.; Scuseria, G. E.; Robb, M. A.; Cheeseman, J. R.; Scalmani, G.; Barone, V.; Mennucci, B.; Petersson, G. A.; Nakatsuji, H.; Li, X.; Caricato, M.; Marenich, A.; Bloino, J.; Janesko, B. G.; Gomperts, R.; Mennucci, B.; Hratchian, H. P.; Ortiz, J. V.; Izmaylov, A. F.; Sonnenberg, J. L.; Williams-Young, D.; Ding, F.; Lipparini, F.; Egidi, F.; Goings, J.; Peng, B.; Petrone, A.; Henderson, T.; Ranasinghe, D.; Zakrzewski, V. G.; Gao, J.; Rega, N.; Zheng, G.; Liang, W.; Hada, M.; Ehara, M.; Toyota, K.; Fukuda, R.; Hasegawa, J.; Ishida, M.; Nakajima, T.; Honda, Y.; Kitao, O.; Nakai, H.; Vreven, T.; Throssell, K.; Montgomery, J. A., Jr.; Peralta, J. E.; Ogliaro, F.; Bearpark, M.; Heyd, J. J.; Brothers, E.; Kudin, K. N.; Staroverov, V. N.; Keith, T.; Kobayashi, R.; Normand, J.; Raghavachari, K.; Rendell, A.; Burant, J. C.; Iyengar, S. S.; Tomasi, J.; Cossi, M.; Millam, J. M.; Klene, M.; Adamo, C.; Cammi, R.; Ochterski, J. W.; Martin, R. L.; Morokuma, K.; Farkas, O.; Foresman, J. B.; Fox, D. J. *Gaussian 09*, revision E.01; Gaussian, Inc.: Wallingford, CT, 2016.
- (30) Zhao, Y.; Truhlar, D. G. The M06 suite of density functionals for main group thermochemistry, thermochemical kinetics, non-covalent interactions, excited states, and transition elements: two new functionals and systematic testing of four M06-class functionals and 12 other functionals. *Theor. Chem. Acc.* **2008**, *120*, 215–241.
- (31) Chai, J.-D.; Head-Gordon, M. Long-range corrected hybrid density functionals with damped atom–atom dispersion corrections. *Phys. Chem. Chem. Phys.* **2008**, *10*, 6615–6620.
- (32) The triple- ζ 6-311+G(d,p) basis set was used throughout as the most complete one available for timely completion of jobs; polarization and diffuse functions were employed to expand the basic basis set to better describe the electron density around the weakly interacting atoms in the cyclic transition states. See refs 33 and 34.
- (33) Boese, A. D.; Martin, J. M. L.; Handy, N. C. The role of the basis set: assessing density functional theory. *J. Chem. Phys.* **2003**, *119*, 3005–3014.
- (34) Lynch, B. J.; Zhao, Y.; Truhlar, D. G. Effectiveness of Diffuse Basis Functions for Calculating Relative Energies by Density Functional Theory. *J. Phys. Chem. A* **2003**, *107*, 1384–1388.
- (35) Check, C. E.; Gilbert, T. M. Progressive Systematic Underestimation of Reaction Energies by the B3LYP Model as the Number of C–C Bonds Increases: Why Organic Chemists Should Use Multiple DFT Models for Calculations Involving Polycarbon Hydrocarbons. *J. Org. Chem.* **2005**, *70*, 9828–9834.
- (36) Grimme, S.; Antony, J.; Ehrlich, S.; Krieg, H. A consistent and accurate ab initio parametrization of density functional dispersion correction (DFT-D) for the 94 elements H–Pu. *J. Chem. Phys.* **2010**, *132*, No. 154104.
- (37) Riplinger, C.; Neese, F. An efficient and near linear scaling pair natural orbital based local coupled-cluster method. *J. Chem. Phys.* **2013**, *138*, No. 034106.
- (38) Riplinger, C.; Sandhoefer, B.; Hansen, A.; Neese, F. Natural triple excitations in local coupled-cluster calculations with pair natural orbitals. *J. Chem. Phys.* **2013**, *139*, No. 134101.
- (39) Riplinger, C.; Pinski, P.; Becker, U.; Valeev, E. F.; Neese, F. Sparse maps – A systematic infrastructure for reduced-scaling electronic structure methods. II. Linear scaling domain based pair natural orbital coupled cluster theory. *J. Chem. Phys.* **2016**, *144*, No. 024109.
- (40) Neese, F. The ORCA program system. *WIREs Comput. Mol. Sci.* **2012**, *2*, 73–78.
- (41) Neese, F. Software update: the ORCA program system, version 4.0. *WIREs Comput. Mol. Sci.* **2018**, *8*, No. e1327.
- (42) Feller, D. The Role of Databases in Support of Computational Chemistry Calculations. *J. Comput. Chem.* **1996**, *17*, 1571–1586.
- (43) Schuchardt, K. L.; Didier, B. T.; Elsethagen, T.; Sun, L.; Gurumoorathi, V.; Chase, J.; Li, J.; Windus, T. L. Basis Set Exchange: A Community Database for Computational Sciences. *J. Chem. Inf. Model.* **2007**, *47*, 1045–1052.
- (44) Pritchard, B. P.; Altarawy, D.; Didier, B.; Gibson, T. D.; Windus, T. L. A New Basis Set Exchange: An Open, Up-to-date Resource for the Molecular Sciences Community. *J. Chem. Inf. Model.* **2019**, *59*, 4814–4820.
- (45) Dennington, R.; Keith, T. A.; Millam, J. M. *GaussView, version 4.1.2*; Semichem Inc.: Shawnee Mission, KS, 2007.
- (46) Schmidt, J. R.; Polik, W. F. *WebMO (Version 19.0)*; WebMO LLC: Holland, MI, 2019 <http://www.webmo.net>.
- (47) *Kaleidagraph for Macintosh, Version 4.5.4*; Synergy Software: Reading, PA, 2018.
- (48) Keith, T. A. *AIMAll, Version 12.06.03*; TK Gristmill Software: Overland Park, KS, 2012.
- (49) Bader, R. F. W. *Atoms in Molecules: A Quantum Theory*; Oxford University Press: Oxford, 1990.
- (50) Bader, R. F. W. A Quantum Theory Of Molecular Structure And Its Applications. *Chem. Rev.* **1991**, *91*, 893–928.

- (51) Bader, R. F. W. Atoms In Molecules. *Acc. Chem. Res.* **1985**, *18*, 9–15.
- (52) Skoog, D. A.; West, D. M.; Holler, F. J. *Fundamentals of Analytical Chemistry*, 7th ed.; Saunders College Publishing: Fort Worth, TX, 1996, Chapters 3 and 4.
- (53) Szilagy, S.; Ross, J. A.; Lemal, D. M. Perfluorotetramethylcyclopentadienone as a Diels–Alder diene. *J. Am. Chem. Soc.* **1975**, *97*, 5586–5588.
- (54) Barlow, M. G.; Haszeldine, R. N.; Pickett, J. A. Heterocyclic polyfluoro-compounds. Part 26. Synthesis of 3,6-bistrifluoromethylpyridazines and -dihydropyridazines. *J. Chem. Soc., Perkin Trans. 1* **1978**, 378–380.
- (55) Kirmse, W.; Mrotzeck, U.; Siegfried, R. Umlagerungen von 5,5,6,6-tetraalkyl-2-norbornyl-kationen. *Chem. Ber.* **1991**, *124*, 241–245.
- (56) Bachrach, S. M.; White, P. B. Towards assessing the aromaticity of the Diels–Alder transition state. *J. Mol. Struct.: THEOCHEM* **2007**, *819*, 72–78.
- (57) Fleming, I. *Frontier Orbitals and Organic Chemical Reactions*; Wiley: London, 1976, Chapter 4.
- (58) Levandowski, B. J.; Abularrage, N. S.; Raines, R. T. Geminal repulsion disrupts Diels–Alder reactions of geminally substituted cyclopentadienes and 4H-pyrazoles. *Tetrahedron* **2021**, *91*, No. 132160.
- (59) Carroll, T. X.; Thomas, T. D.; Bergersen, H.; Børve, K. J.; Sæthre, L. J. Fluorine as a π Donor. Carbon 1s Photoelectron Spectroscopy and Proton Affinities of Fluorobenzenes. *J. Org. Chem.* **2006**, *71*, 1961–1968.
- (60) Wiberg, K. B.; Rablen, P. R. Substituent Effects. 7. Phenyl Derivatives. When Is a Fluorine a π -Donor? *J. Org. Chem.* **1998**, *63*, 3722–3730.